

Scuola di Specializzazione in Radiodiagnostica

Direttore: Prof. Davide Caramella



Tesi di Specializzazione

**ROLE OF ADVANCED MR TECHNIQUES IN
PREDICTING RESPONSE TO CHEMORADIOTHERAPY
IN GLIOBLASTOMAS**

Relatori:

Chiar.mo Prof. Davide Caramella

Prof. Mirco Cosottini

Candidata:

Dott.ssa Ilaria Desideri

Anno Accademico 2014/2015

INDEX

ABSTRACT	pag. 3
INTRODUCTION	pag. 5
MATERIALS AND METHODS	pag. 6
RESULTS	pag. 14
DISCUSSION	pag. 16
CONCLUSIONS	pag. 23
REFERENCES	pag. 24

Abstract

Background and purpose

For patients with glioblastomas the standard therapy is represented by maximal safe tumor resection followed by concurrent chemoradiotherapy with temozolomide (TMZ) and adjuvant TMZ. Determination of the response to therapy is entirely dependent on the interpretation of magnetic resonance (MR) imaging findings and clinical manifestations.

The purpose of this study was to assess the utility of MR advanced techniques such as diffusion (DWI) and perfusion (PWI) imaging in predicting response or progression of gliomas to chemoradiotherapy.

Materials and methods

We retrospectively selected 32 patients with high grade glioma treated with surgical resection followed by radiation therapy and temozolomide who underwent conventional MR imaging and advanced MR techniques before surgery (T_0), before (T_1) and after RT (T_2). By using the RANO criteria at T_2 , the patients were divided into two groups, “progression” and “response”. Pre and postcontrastographic T1-weighted images were coregistered with the Apparent Diffusion Coefficient (ADC) and PWI maps . Contrast Enhancement, permeability (PSR), minimum value of ADC and maximum value of relative Cerebral Blood Volume (rCBV) were calculated with a ROI method at T_0 , T_1 and T_2 and used as variables. In conventional MRI we calculated the incremental ratio of the size of the pre and post operative tumor.

Unpaired t-test was used to test difference between groups for the above-mentioned variables for each time point. Significant data were utilized in the

univariate logistic regressions in order to determine odds ratios for assessing risk factors. A multivariate logistic regression was performed on univariate significant variables.

Results

At unpaired t-test ADC, PSR and rCBV at T₁ presented statistical significant differences between the two groups. For the group “progression” the univariate logistic regressions with these variables, adjusted for gender and age, identified ADC and rCBV as predictors of progression while in the subsequent multivariate logistic regression only ADC showed statistical significance as predictor. For the group “response” the univariate logistic regressions with these variables, adjusted for gender and age, identified ADC, rCBV and PSR as predictors of response while in the subsequent multivariate logistic regression only PSR showed statistical significance.

Conclusions

MR advanced techniques, in particular diffusion with ADC and perfusion with PSR, have proved a valuable aid in predicting respectively progression and response of glioblastomas to chemoradiotherapy.

Introduction

Glioblastoma multiforme (GBM) is the most common primary malignant brain tumor in adults, accounting for approximately one percent of all tumors. Despite the evaluation of multiple treatment approaches, the prognosis for patients with GBM is still extremely poor, with an estimated median survival of 9-18 months [1,2]. Currently, maximal safe tumor resection followed by concurrent chemoradiotherapy (CCRT) with temozolomide (TMZ) and adjuvant TMZ is the standard therapy for patients with GBM [3]. Determination of the response to therapy is entirely dependent on the interpretation of magnetic resonance (MR) imaging findings and clinical manifestations [4].

In 1990, Macdonald introduced radiological and clinical response criteria for malignant brain tumours [5]. These criteria provide a standardized radiological assessment of the tumour response and are based on measuring the enhancing component of the tumour. The enhancing portion of GBM is a key factor for using these criteria to predict the prognosis of GBM patients. Furthermore, in 2010, the Response Assessment in NeuroOncology (RANO) Working Group proposed new standardized criteria for accurately assessing the tumor response in high-grade glioma patients [6]. The RANO criteria emphasize not only the evaluation of the non-enhancing component but also precise examination of measurable enhancing tumor components. The measurable enhancing lesions are defined as bidimensionally contrast-enhancing lesions with clearly defined margins by computed tomography (CT) or MRI scans and two perpendicular diameters of at least 10 mm visible on two or more axial slices that are preferably, at most, 5 mm apart with 0-mm skip [6,7].

The use of these criteria allows to establish the presence of progression or response only after chemoradiotherapy.

The availability of predictors of progression or response before starting the therapy would be helpful to know patient prognosis [8], to avoid futile care and to reduce the risk of any side effects to the patient.

In recent years several genetic markers able to predict the response of the patient to therapy have been identified [9-11].

Also MR imaging with advanced techniques has been tested, trying to predict the prognosis for patients with high-grade glioma [12-18].

The purpose of this study was to assess the utility of DWI and DSC perfusion imaging in predicting response or progression of glioma to chemoradiotherapy.

Materials and Methods

Patient selection criteria and clinical data collection

In this retrospective study the patient cohort consisted in 32 patients with High Grade Glioma (HGG) according to the following inclusion criteria: 1) histological diagnosis of glioblastoma or anaplastic astrocytoma obtained on surgical specimen performed in our center, 2) treatment with RT and temozolamide, 3) brain MRI imaging, including contrast T1-weighted imaging, DWI and/or DSC perfusion before surgery (T_0), after surgery before RT (T_1) and after RT (T_2).

The lack of one of the mentioned criteria constitutes cause of exclusion from the retrospective study.

The 32 patients were 22 women and 10 men with median age of 55.1 years (range 27-78 years). All patients were affected by HGG, in particular by glioblastoma (n = 84.4%) and anaplastic astrocytoma (n =15.6%).

At initial diagnosis, patients underwent gross total resection of the tumours (n=7) or partial resection of the tumour (n=16).

Radiotherapy consisted of fractionated focal irradiation at a dose of 2 Gy per fraction given once daily five days per week over a period of six weeks, for a total dose of 60 Gy. Radiotherapy was delivered to the gross tumour volume with a 2-to-3-cm margin for the clinical target volume. Radiotherapy was planned with dedicated computed tomography (CT) and three-dimensional planning systems; conformal radiotherapy was delivered with linear accelerators with nominal energy of 6 MV or more, and quality assurance was performed by means of individual case reviews. All patients received concomitant temozolomide at standard dose.

Patients were followed along the time to register clinical changes and to determine overall survival.

The patients were divided into two main groups, “progression” and “response” groups, on the basis of RANO criteria applied at T₂ and in subsequent follow-up MR examinations. According to these criteria 17 patients were identified as belonging to group “progression” and 12 patients belonging to group “response”. 3 patients were classified in a separate group denominated “pseudoprogression”, on the basis of the behaviour of the enhancing lesion in the post- radiotherapy period. These patients had a worsening of the neuroradiological picture at T₂ with a tumoural regression in the subsequent MR examination.

MRI examination protocol and Image evaluation

Conventional MRI

MRI examinations were performed on 1.5 T and 3 T MR system (Signa and Discovery 750, GE Healthcare, Milwaukee, Wisconsin) with a quadrature head coil. After triplanar scout view, the MRI examination protocol consists of pre-contrast conventional MRI followed by DWI, MRS and PWI, and finally post-contrast T1 weighted images.

Conventional MR examination consisted in axial fluid-attenuated inversion recovery images (FLAIR, TR 10000 msec, TE 100 msec, TI 2000 msec, FOV 24 cm, Tk 5 mm, gap 1 mm, NEX 1, matrix 192 x 256, acquisition time 4'35''), axial spin-echo T1-weighted (TR 500 msec, TE 9.4 msec, FOV 22, Tk 4 mm, gap 1 mm, NEX 2) and axial fast spin-echo T2-weighted (TR 4930 msec, TE 104 msec, FOV 22, Tk 4 mm, gap 1 mm, NEX 2) images. After contrast media administration high resolution volumetric images with T1-weighted SPGR sequence (TR 2160 msec, TE 3.9 msec, TI 1100 msec, FOV 25.6, Tk 1.2 mm, gap 0 mm, NEX 1) and spin echo axial T1 weighted sequences were obtained.

Post contrast T1-weighted images and T2-weighted images were used to apply RANO criteria in order to group patients in “progression” and “response”. In particular patients who met any one of following criteria were classified as having progressive disease: (a) >25% increase in the sum of the products of the perpendicular diameters of enhancing lesions with the smallest tumor measurement; (b) any new lesion; (c) clear clinical deterioration not attributable to other causes apart from the tumor; (d) failure to return for evaluation as a result of death or deteriorating condition; and (e) clear progression of non-measurable disease.

Axial precontrast and post contrast T1-weighted images were subsequently coregistered and the section containing the maximum diameter of the enhancing lesion was selected for subsequent ROI analysis. We drew a small circular ROI in the enhancing lesion to obtain the highest signal value (S) and we duplicate the circular ROI in the same region of pre-contrast image (S0). These values were then used to calculate the Contrast Enhancement (CE) = $S - S_0/S_0$ as incremental ratio.

By using conventional MRI we also calculated the incremental ratio of the size of the pre and post operative tumour. In axial postcontrast T1-weighted image at T0 we obtained tumoral size considering only measurable lesions according to RANO criteria (enhancing lesions with diameter >1cm) multiplying the largest diameter to the diameter perpendicular to it (Figure 1). We used a similar procedure to measure tumoral size in the postcontrast T1 weighted image at T1 after surgery. Then using the formula $((\text{sizeT0} - \text{sizeT1})/\text{sizeT0})$ we obtained incremental ratio of tumoral size.

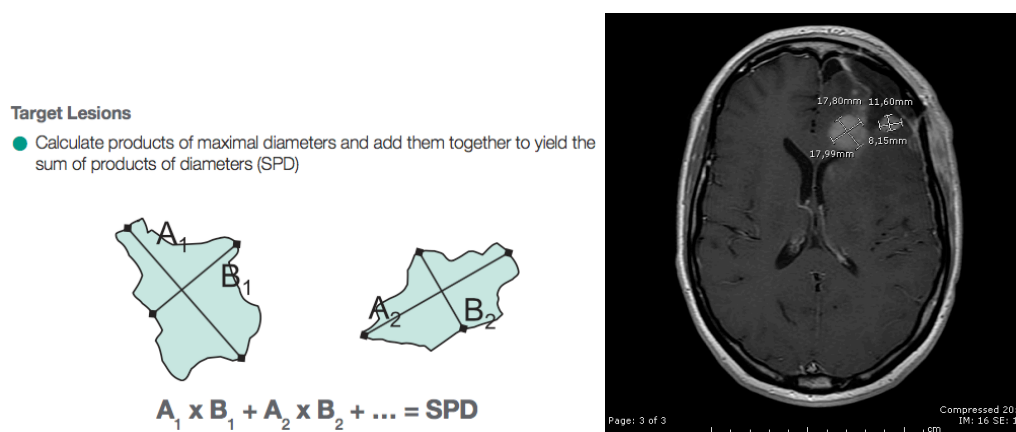


Figure 1. Application of RANO criteria for measurable lesions. Tumoural size is obtained multiplying the largest diameter to the diameter perpendicular to it.

DWI

DWIs were acquired before contrast media administration using echoplanar imaging (EPI) sequences (TR 4300, TE 97, FOV 24, thickness 4 mm, spacing 1,2 mm, NEX 3, matrix 128 x 128, acquisition time 1'15'') implemented by diffusion gradients ($b = 0, 1000 \text{ s/mm}^2$) in three or six orthogonal directions.

The DWI data were transferred together with the anatomic data to a workstation (Advantage Workstation, GE Healthcare) and were analysed by using commercial software (FuncTool, GE Healthcare). ADC maps were calculated and coregistrated with the axial precontrast and post contrast T1-weighted images and with Cerebral Blood Volume (CBV) maps. The contrast images were inspected and the section containing the maximum diameter of the enhancing lesion was selected for subsequent ROI analysis. We drew a small circular ROI (approximately 20 mm^2) within the enhancing lesion that was adjusted onto the ADC map as necessary to target areas with visually low ADC values; the value obtained was recorded as ADC_{ROI} . The ADC ratio was calculated by dividing the ADC_{ROI} by the ADC value obtained from measuring a similar small circular ROI in the contralateral normal brain of contralateral hemisphere (Figure 2).

DSC Perfusion

PWI images were obtained with an axial T2* weighted gradient EPI sequence (TR 2000 msec, TE 90 msec, FA 30, FOV 34 cm, tk 5mm, spacing 1 mm, matrix 128 x 128, 40 phases for slice, 12 slices and acquisition time 1.14 min). Contrast media (gadolinium chelate) bolus injection started after the completion of the tenth acquisition at a flow rate of 5 ml/sec for a total of 14

ml using a 18 Gauge venous access connected to an automatic injector Spectris Medrad. Before the PWI acquisition a prebolus of 2 ml of gadolinium chelate was administered to compensate the alteration of the blood-brain barrier that is present in some tumours.

The DSC data were transferred together with the anatomic data to a workstation (Advantage Workstation, GE Healthcare) and were analysed by using commercial software (FuncTool, GE Healthcare). T2*-weighted signal intensity-time curves were derived on a voxel-by-voxel basis. Post hoc correction for leakage was performed by using γ -variate curve fitting to approximate the curve without recirculation and leakage. Cerebral blood volume maps were calculated and coregistered with the axial precontrast and post contrast T1-weighted images and with ADC maps. ROI analysis for CBV was performed with the same method described for ADC.

We drew a small circular ROI (approximately 20 mm²) within the enhancing lesion that was adjusted onto as necessary to target areas with visually highest CBV; the value obtained was recorded as CBV_{ROI}. The relative CBV (rCBV) was calculated by dividing the CBV_{ROI} by the CBV value obtained from measuring a similar small circular ROI in the contralateral normal brain of contralateral hemisphere (Figure 2).

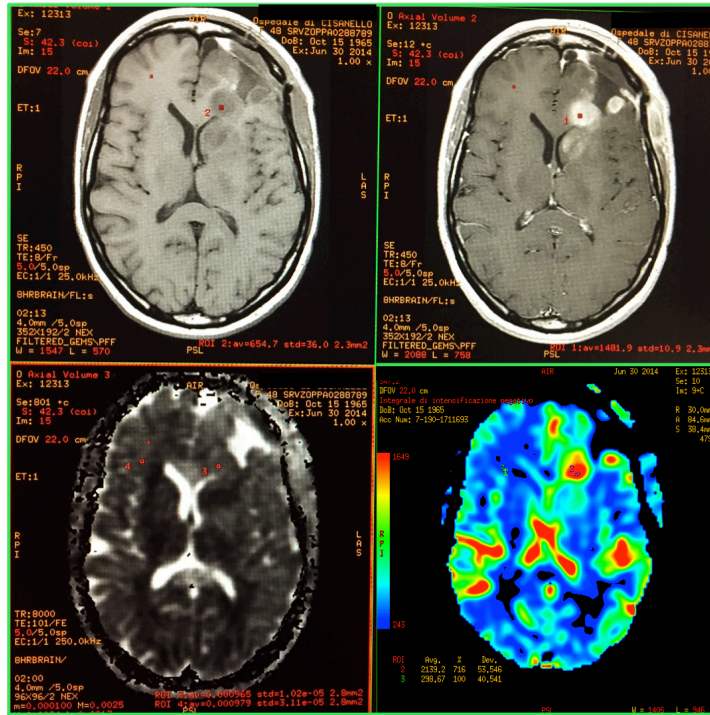


Figure 2. Coregistration of ADC maps, axial precontrast and post contrast T1-weighted images and CBV maps. ROIs were positioned in the section containing the maximum diameter of the enhancing lesion.

The signal intensity-time curve of the CBV_{ROI} was also used to calculate the permeability by determining S_0 = precontrast baseline signal intensity, S_{min} = minimum signal intensity at the peak of contrast bolus and S_1 = end signal intensity at 50 seconds (Figure 3). These values were then used to calculate the Percentage Signal Recovery (PSR) as follow: $PSR = (S_1 - S_{min}) / (S_0 - S_{min})$.

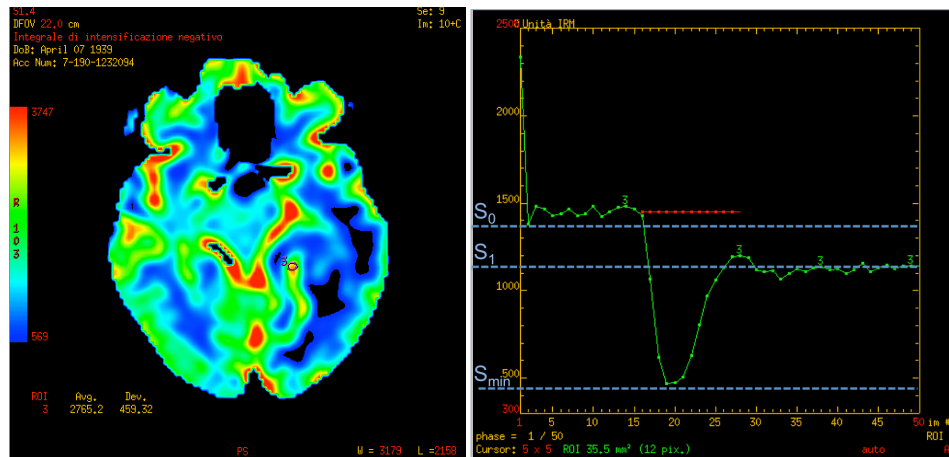


Figure 3. CBV ROI positioned in the CBV map (left) with the correspondent signal intensity-time curve, on which PSR was calculated (right).

Statistical Analysis

Statistical analysis was conducted with R (www.R-project.org/). The results with p values of < 0.05 were considered statistically significant.

Unpaired t-test was used to test difference between progression and responding groups for variable : ADC ratio, CE, PSR, rCBV at time T_0 , T_1 and T_2 . We also tested age, incremental ratio of tumor dimensions $((\text{size}T_0 - \text{size}T_1)/\text{size}T_0)$ and duration of radiotherapy. Fisher's exact test was performed on categorical variable such a gender.

Significative data were utilized in the univariate logistic regressions adjusted for gender and age in order to determine odds ratios (with 95% confidence interval) for assessing risk factors. Finally, a multivariate logistic regression was performed on univariate significant variables.

Results

The variables ADC ratio, rCBV, CE and PSR were calculated at T_0 (before surgery), T_1 (before RT) and T_2 (after RT).

Unpaired t-test was used to test difference between groups for above mentioned variables for each time point, in addition to age, to the incremental ratio of the size of the pre and post operative tumor and to the duration of RT. The t-test presented statistical significant differences between the groups “progression” and “response” at T_1 for the variables ADC ratio, PSR and rCBV (*p value* respectively of 0.03, 0.007 and 0.01) (Figure 4). The other variables at T_1 and the variables calculated at T_0 and T_2 did not present statistical significant differences between the groups.

The group “pseudoprogression” was not statistically tested because of the small number of patients.

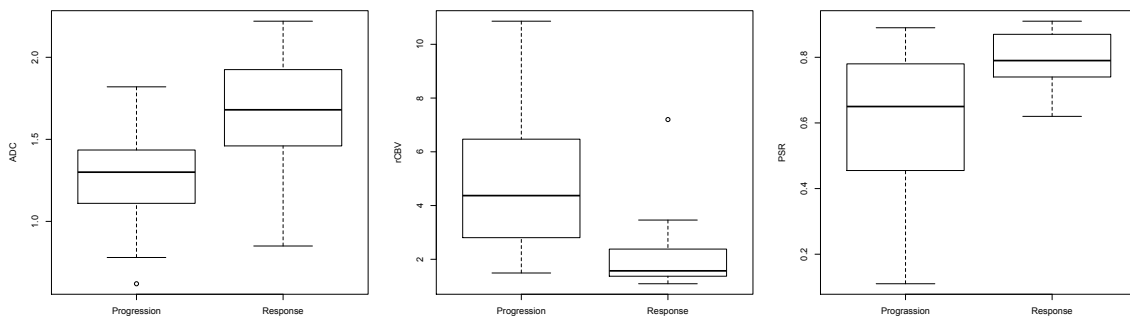


Figure 4. Box-plots represent significant differences between the groups “progression” and “response” respectively for ADC ratio, rCBV and PSR.

The significant data were utilized in the univariate logistic regression in order to determine odds ratios (OR) for assessing risk factors.

For the group “progression” the univariate analysis with these variables, adjusted for gender and age, identified ADC ratio and rCBV as predictors of progression.

In particular, ADC ratio ($p = 0.03$) presented an OR at 0.080 with a confidence interval (C.I.) of 0.008-0.054, while rCBV ($p = 0.05$) presented an OR at 1.48 with a C.I. of 0.999-2.198.

The two predictors mentioned above were used in multivariate analysis, in which ADC ratio remained the strongest predictor of progression ($p = 0.05$) with an OR at 0.057 with a C.I. of 0.003-1.009 (Figure 5).

For the group “response” the univariate analysis with the same variables, adjusted for gender and age, identified ADC ratio, rCBV and PSR as predictors of response. In particular, ADC ratio ($p = 0.04$) presented an OR at 11.06 with a C.I. of 1.041-117.616, rCBV ($p = 0.03$) presented an OR at 0.56 with a C.I. of 0.335-0.962 and PSR ($p = 0.04$) presented an OR at 1.00 with a C.I. of 1.000-1.017. In the subsequent multivariate analysis with these three predictors, PSR remained the strongest predictor of response ($p = 0.04$) with an OR at 1.01 with a C.I. of 1.000-1.024 (Figure 6).

Variables	Progression					
	Age- and gender- adjusted			Multivariate-adjusted		
	OD	95% CI	<i>p</i> value	OD	95% CI	<i>p</i> value
ADC ratio	0.080	0.008-0.054	0.036	0.057	0.003-1.009	0.050
rCBV	1.48	0.999-2.198	0.050	1.346	0.817-2.220	0.244
PSR	0.99	0.987-1.000	0.059	0.993	0.986-1.000	0.066
Gender	---	---	---	0.958	0.876-1.048	0.348
Age	---	---	---	0.797	0.083-7.615	0.844

Figure 5. Age- and gender-adjusted and multivariate-adjusted odds ratio and 95% confidence intervals of variables for the group “progression”.

Variables	Response					
	Age- and gender- adjusted			Multivariate-adjusted		
	OD	95% CI	<i>p</i> value	OD	95% CI	<i>p</i> value
ADC ratio	11.64	1.041-117.616	0.046	36.62	0.782-1713.15	0.066
rCBV	0.567	0.335-0.962	0.035	0.550	0.263-1.148	0.111
PSR	1.008	1.000-1.0170	0.043	1.012	1.000-1.024	0.042
Gender	---	---	---	0.973	0.055-17.189	0.985
Age	---	---	---	1.060	0.937-1.200	0.348

Figure 6. Age- and gender-adjusted and multivariate-adjusted odds ratio and 95% confidence intervals of variables for the group “response”.

Discussion

The RANO criteria were proposed in 2010 by the RANO Working Group with the purpose of overcoming the limitations of previous Macdonalds criteria [6]. The main innovations consist in the introduction of nonenhancing lesions (only observable in T2-weighted images) in the evaluation of MR images and in adding a better definition of how to take measurements of enhancing lesions.. Currently this type of evaluation, in association with the clinical condition of the patient, determines whether there has been a progression of the disease, a partial response, a complete response or stability of the disease.

The RANO criteria also introduce the assessment of the effects of chemoradiotherapeutic treatment, in particular the phenomena of pseudoprogression and pseudoresponse [6].

Pseudoprogression is a subacute treatment-related change characterized by a transient increase of contrast enhancement, after irradiation and chemotherapy with temozolomide, in the absence of tumor. It usually develops <6 months

after RT with self-limited enhancing lesions that spontaneously stabilize and resolve within 2-6 months without any new treatment [19]. This phenomenon is most likely induced by a pronounced local tissue reaction with an inflammatory component, oedema and abnormal vessel permeability causing new or increased contrast enhancement on MR imaging examinations [20]. Transient increases in contrast enhancement just after completion of chemoradiotherapy play an important role in clinical management of patients with cancer because they complicate the ability of physician to determine whether to continue with standard adjuvant chemotherapy or to switch to a second-line therapy for recurrence. Thus, the detection of pseudoprogression versus true progression is a critical important issue in oncology practice [20].

In our cohort of patients we have identified 3 patients with pseudoprogression, in which we observed the appearance of an enhancing lesion at MR imaging at T₂ after 1 month of the end of RT with net reduction or complete disappearance in the subsequent MR controls (Figure 7).

Because of the small number of these patients, it was not possible to perform statistical tests to determine the role of the advanced MR techniques in the differential diagnosis between pseudoprogression and progression neither to test if advance MR parameters might constitute a predictor for future development of pseudoprogression.

However, several studies have revealed that advanced MR techniques allow to differentiate pseudoprogression and true progression. Mangla et al. [21] and Tsien et al. [22] demonstrated a reduction in rCBV in patients with pseudoprogression and an increase in rCBV in tumor progression. Prager et al. [19] found higher diffusion and lower perfusion values in treatment-related changes, and in particular in pseudoprogression, than in recurrent tumour, in patients with HGGs and these results reflect the lower cellularity and vascularity of treatment-related changes, respectively, and suggest that DWI

and DSC perfusion are useful tools in discriminating treatment-related changes from recurrent tumour.

The above-mentioned characteristics were identified also in 3 patients of our cohort (Figure 7).

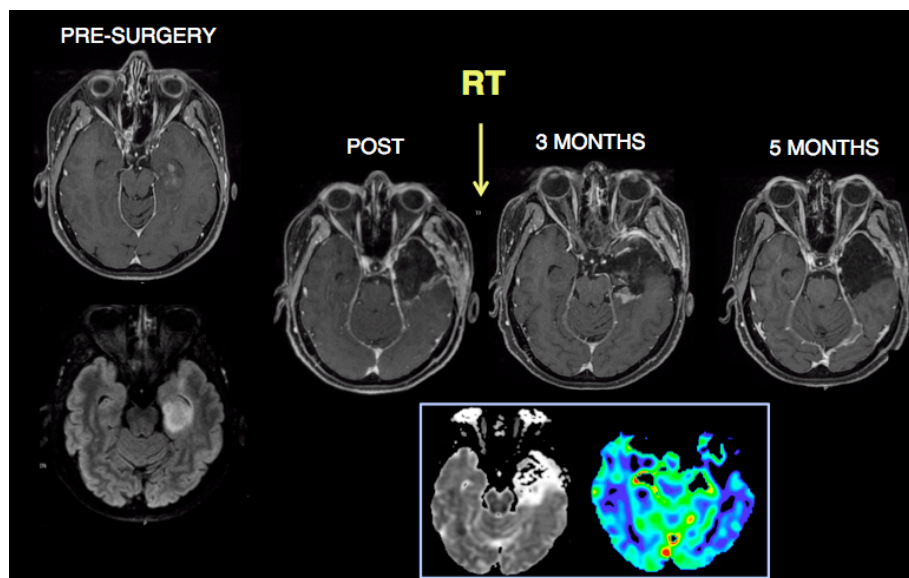


Figure 7. A case of pseudoprogression. Appearance of an enhancing lesion at MR imaging after about 1 month after the end of RT with complete disappearance in the subsequent MR control.

With regard to the phenomenon of pseudoresponse, antiangiogenic agents, especially those targeting vascular endothelial growth factor (VEGF), such as bevacizumab, and the VEGF receptor, such as cediranib, can produce marked decrease in contrast enhancement as early as 1 to 2 days after initiation of therapy and commonly result in high radiologic response rates of 25% to 60% [23-26]. These apparent responses to antiangiogenic therapy may be partly a result of normalization of abnormally permeable tumor vessels and not always necessarily indicative of a true antiglioma effect. As a result, radiologic responses in studies with antiangiogenic agents should be interpreted with caution. For this reason, the RANO criteria suggest that radiologic responses should persist for at least 4 weeks before they are considered as true responses [6].

In our cohort, one patient receiving bevacizumab presented pseudoresponse. In this patient, the decrease of contrast enhancement and of rCBV after the initiation of the therapy could be interpreted as a response, but at T2-weighted images we observed an extensive neoplastic diffusion with bilateral nonenhancing and not measurable lesions, confirmed by MR Spectroscopy Imaging (Figure 8).

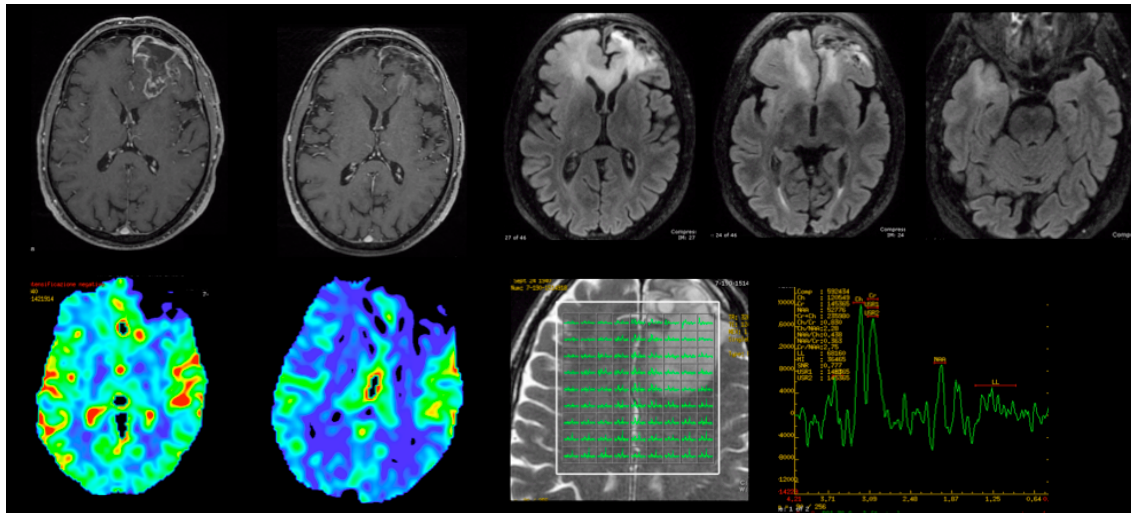


Figure 8. A case of pseudoresponse. Reduction of contrast enhancement and of rCBV after therapy; in T2-weighted images, extensive neoplastic diffusion with bilateral nonenhancing and not measurable lesions, confirmed by MR Spectroscopy Imaging extends beyond the corpus callosum indicating tumour progression despite the disappearance of contrast enhancement.

The RANO criteria allows to establish the presence of progression or response only after chemoradiotherapy.

In recent years various prognostic genetic markers have been identified in GBM, including methylation status of the gene promoter for O⁶-methylguanine-DNA methyltransferase (MGMT), isocitrate dehydrogenase enzyme 1/2 (IDH1/2) mutation, epidermal growth factor receptor (EGFR) overexpression and amplification, glioma-CpG island methylator phenotype (G-CIMP), tumor protein (TP53) mutation and genetic losses of chromosomes

[27]. For example, it has been amply demonstrated that methylation of MGMT causes silencing of the gene and interference with DNA repair and increases TMZ sensitivity while an unmethylated promoter for *MGMT*, results in active gene expression and high levels of the repair enzyme that results in chemotherapy resistance [28,29]. It is also known that IDH1 mutated high grade gliomas arise by transformation from lower-grade gliomas and have distinguishing radiographic, histologic and transcriptional features (frontal location and lesser extent of contrast enhancement and necrosis) that are consistent with a less aggressive clinical course. IDH1 mutated high grade gliomas have a more favourable prognosis than the ones without IDH1 mutation [27,30].

The results of the present study suggest that MR advanced techniques allow us to identify some predictors of response or progression to chemoradiotherapy in patients with High Grade Gliomas, in particular DWI and DSC perfusion at T₁ or rather in the MR examination after surgery and before the start of the therapy.

Diffusion and perfusion MR imaging provides physiologic information that is not available with conventional MR imaging [19]. DWI measures the motility of water molecules and alterations in the balance of intracellular and extracellular water restricted by cell membranes and other structures. Areas of diffusion restriction in tumours are correlated with increased tumour cellularity [31]. The greater is the cellularity of the tumour and the lowest is the ADC value, because the diffusivity of water is reduced in consequence of the relative decrease of the extracellular space for the movement of protons. Studies carried out by Bulakbasi et al [32], Fan et al [33] and Arvinda et al [34] have shown that there is inverse correlation between the degree of gliomas and ADC: higher is the tumour cellularity and grade of glioma, lower is the ADC value.

DSC MR perfusion is an advanced technique that provides independent

information on neoangiogenesis, vascular attenuation, and microvascular leakiness [20,21]. These features are indicative of the aggressiveness of tumors and, as demonstrate by several studies, high-grade gliomas have a greater degree of perfusion and rCBV compared to those low-grade, due to a major neoangiogenesis [34-40].

In recent years, some authors have tried to determine if MR advanced techniques can be used to predict the patient response to concurrent chemoradiotherapy with temozolomide, evaluating contrast-enhancing lesions detected on immediate post-operative MR imaging. Lee et al [41] showed that the normalized CBV (nCBV) on immediate post-operative MR imaging was significantly higher in the progression group than in the non-progression group ($p = 0.033$) and so it may be feasible for predicting glioblastoma response to chemoradiotherapy with temozolomide. In the mentioned-above study normalized ADC and other parameters evaluated showed no significant differences between the two groups and the could not be used to predict the treatment response. Kim et al [42] showed that nCBV value can be used for the prognosis prediction of a measurable enhancing lesion after the completion of standard treatment for GMB, wherein a high 99th percentile nCBV value (>4.5) suggests a better PFS for GBM patients. Conversely, a low 99th percentile nCBV values seem to indirectly reflect hypoxic conditions, which could make cancer cells more aggressive and resistant to treatment. Also in this study ADC was not significantly different between the two groups.

In our study, for the group “progression” the univariate analysis, adjusted for gender and age, identified ADC ratio and rCBV as predictors of progression with OD respectively of 0.080 and 1.48 and C.I. respectively of 0.008-0.054 and 0.999-2.198. In the subsequent multivariate analysis only ADC ratio remained the strongest predictor of progression ($p = 0.05$) with an OR at 0.057 with a C.I. of 0.003-1.009.

According to the results of our study, a low ADC ratio at T1 before the initiation of therapy implicate a higher probability of a progression of the disease after chemoradiotherapy.

For the group “response” the univariate analysis, adjusted for gender and age, identified ADC ratio, rCBV and PSR as predictors of response with OD respectively of 11.06, 0.56 and 1.00 and C.I. respectively of 1.041-117.616, 0.335-0.962 and 1.000-1.017. In the subsequent multivariate analysis only PSR remained the strongest predictor of response ($p = 0.04$) with an OR at 1.01 with a C.I. of 1.000-1.024.

PSR is a measure of permeability influenced by leakage of contrast and the size of the extravascular space, with lower PSR reflecting higher permeability [19]. Capillary permeability is another feature of angiogenesis in high-grade gliomas. PSR, obtained from a DSC perfusion MR technique, gives similar information to K^{trans} obtained with DCE perfusion, which is an estimation of the capillary permeability based on measuring the contrast leakage rate between the intravascular and extravascular spaces. Several studies showed that it generally correlates with histological grading and length of survival in gliomas [43-47].

According to the results of our study a high value of PSR at T1 before the initiation of therapy implicate a higher probability of a response of the patients after chemoradiotherapy.

Apart from the intrinsic limits of any retrospective study, a number of other limitations of the present study should be mentioned. First, this study included a small number of patients and this might have resulted in selection bias. The small number of the patients is due to the rigidity of the inclusion criteria; furthermore, often follow-up examinations are not performed in the same centre and, if performed in periferic centres, perfusional study is not present.

Therefore, large population studies are required to validate our results. Second, we used multiple MRI scanners with different field strength (1.5 and 3.0 T scanners) and the scan parameters are slightly different for each machine. Although we normalized the CBV and ADC values to minimize the effects of the different magnetic field strengths, there could be a slight bias in the image analysis of the ADC and CBV maps.

Conclusions

MR advanced techniques, in particular diffusion with ADC and perfusion with PSR, have proved a valuable aid in predicting respectively progression and response of glioblastomas to chemoradiotherapy.

References

1. Jeon HJ, Kong DS, Park KB et al. Clinical outcome of concomitant chemoradiotherapy followed by adjuvant temozolomide therapy for glioblastomas: single-center experience. *Clin Neurol Neurosurg* 2009; 111:679-682
2. Erpolat OP, Akmansu M, Goksel F et al Outcome of newly diagnosed glioblastoma patients treated by radiotherapy plus concomitant and adjuvant temozolomide: a long-term analysis. *Tumori* 2009; 95:191-197
3. Stupp R, Mason WP, van den Bent MJ et al. Radiotherapy plus concomitant and adjuvant temozolomide for glioblastoma. *N Engl J Med* 2005; 352:987-996
4. Song YS, Choi SH, Park CK et al. True Progression versus Pseudoprogression in the treatment of Glioblastomas: A Comparison Study of Normalized Cerebral Blood Volume and Apparent Diffusion Coefficient by Histogram Analysis *Korean J Radiol* 2013; 14(4):662-672
5. Macdonald DR, Cascino TL, Shold SC Jr, Cairncross JG Response criteria for phase II studies of supratentorial malignant glioma *J Clin Oncol* 1990; 8:1277-1280
6. Wen PY, Macdonald DR, Reardon DA, et al. Updated response assessment criteria for high-grade gliomas: response assessment in neuro-oncology working group. *J Clin Oncol* 2010;28:1963–72

7. Kim JH, Choi SH, Ryoo I et al Prognosis Prediction of Misurable Enhancing Lesion after Completion of Standard Concomitant Chemoradiotherapy and Adjuvant Temozolomide in Glioblastoma Patients: Application of Dynamic Susceptibility Contrast Perfusion and Diffusion Weighted Imaging *PLOS ONE* November 2014
8. Umesh S, Tandon A, Santosh V et al Clinical and immunohistochemical prognostic factors in adult glioblastoma patients *Clinical Neuropathology*, 28:362 - 372
9. Thakkar JP, Dolecek TA, Horbinski C et al Epidemiologic and Molecular Prognostic Review of Glioblastoma *Cancer Epidemiol Biomarkers Prev.* 2014 October ; 23(10): 1985–1996.
10. Collins VP, Ichimura K, di Y et al Prognostic and predictive markers in recurrent high grade glioma; results from the BR12 randomised trial *Acta Neuropathologica Communications* 2014, 2:68
11. Dae Cheol Kim, Ki Uk Kim, Young Zoon Kim Prognostic Role of Methylation Status of the *MGMT* Promoter Determined Quantitatively by Pyrosequencing in Glioblastoma Patients *J Korean Neurosurg Soc* 59 (1) : 26-36, 2016
12. Gahramanov S, Muldoon LL, Varallyay CG et al.. Pseudoprogression of glioblastoma after chemo- and radiation therapy: diagnosis by using dynamic susceptibility-weighted contrast-enhanced perfusion MR imaging with ferumoxytol versus gadoteridol and correlation with survival. *Radiology* (2013) 266: 842–852.
13. Hein PA, Eskey CJ, Dunn JF, Hug EB Diffusion-weighted imaging in the follow-up of treated high-grade gliomas: tumor recurrence versus radiation injury. *AJNR Am J Neuroradiol* (2004) 25: 201–209.

14. Asao C, Korogi Y, Kitajima M, Hirai Tet al.. Diffusion-weighted imaging of radiation- induced brain injury for differentiation from tumor recurrence. *AJNR Am J Neuroradiol* (2005) 26: 1455–1460.
15. Barajas RF Jr, Chang JS, Segal MR et al. Differentiation of recurrent glioblastoma multiforme from radiation necrosis after external beam radiation therapy with dynamic susceptibility-weighted contrast-enhanced perfusion MR imaging. *Radiology* (2009) 253: 486–496.
16. Hu LS, Baxter LC, Smith KA et al. Relative cerebral blood volume values to differentiate high-grade glioma recurrence from posttreatment radiation effect: direct correlation between image-guided tissue histopathology and localized dynamic susceptibility-weighted contrast- enhanced perfusion MR imaging measurements. *AJNR Am J Neuroradiol* (2009) 30: 552–558.
17. Hilario A, Ramos A, Perez-Nunez A et al. The added value of apparent diffusion coefficient to cerebral blood volume in the preoperative grading of diffuse gliomas. *AJNR Am J Neuroradiol* (2012) 33: 701–707.
18. Arvinda HR, Kesavadas C, Sarma PS et al. Glioma grading: sensitivity, specificity, positive and negative predictive values of diffusion and perfusion imaging. *J Neurooncol* (2009) 94: 87–96.
19. Prager AJ, Martinez N, Beal k et al Diffusion and Perfusion MRI to Differentiate Treatment-related Changes including Pseudoprogression from Recurrent Tumors in High-Grade Gliomas with Histopathologic Evidence *AJNR Am J Neuroradiol* January 2015
20. Hygino da Cruz LC Jr, Rodriguez I, Domingues RC et al. Pseudoprogression and pseudoresponse: imaging challenges in the assessment of posttreatment glioma. *AJNR Am J Neuroradiol* 2011;32: 1978 – 85
21. Mangla R, Singh G, Ziegelitz D et al Changes in relative cerebral blood

volume 1 month after radiation-temozolomide therapy can help predict overall survival in patients with glioblastoma. *Radiology* 2010; 256:575-84

22. Tsien C, Galban CJ, Chenevert TL et al Parametric response map as an imaging biomarker to distinguish progression from pseudoprogression in high-grade glioma *J Clin Oncol* 2010; 28:2293-99

23. Batchelor T, Sorensen A, di Tomaso E, et al: AZD2171, a pan-VEGF receptor tyrosine kinase inhibitor, normalizes tumor vasculature and alleviates edema in glioblastoma patients. *Cancer Cell* 11:83- 95, 2007

24. Vredenburgh JJ, Desjardins A, Herndon JE 2nd, et al: Bevacizumab plus irinotecan in recurrent glioblastoma multiforme. *J Clin Oncol* 25:4722- 4729, 2007

25. Friedman HS, Prados MD, Wen PY, et al: Bevacizumab alone and in combination with irinotecan in recurrent glioblastoma. *J Clin Oncol* 27:4733-4740, 2009

26. Kreisl TN, Kim L, Moore K, et al: Phase II trial of single-agent bevacizumab followed by bevacizumab plus irinotecan at tumor progression in recurrent glioblastoma. *J Clin Oncol* 27:740-745, 2009

27. Thakkar JP , Dolecek TA, Horbinski C et al Epidemiologic and Molecular Prognostic Review of Glioblastoma 2014 *Cancer Epidemiol Biomarkers Prev.* 23(10): 1985–1996.

28. Nakagawachi T, Soejima H, Urano Tet al. Silencing effect of CpG island hypermethylation and histone modifications on O6-methylguanine-DNA methyltransferase (MGMT) gene expression in human cancer. *Oncogene.* 2003; 22:8835–8844.

29. Horbinski C. What do we know about IDH1/2 mutations so far, and how do

we use it? *Acta Neuropathol.* 2013; 125:621–636.

30. Lai A, Kharbanda S, Pope WB et al. Evidence for sequenced molecular evolution of IDH1 mutant glioblastoma from a distinct cell of origin. *J Clin Oncol.* 2011; 29:4482–4490.

31. Hein PA, Eskey CJ, Dunn JF, et al. Diffusion-weighted imaging in the follow-up of treated high-grade gliomas: tumor recurrence versus radiation injury. *AJNR Am J Neuroradiol* 2004;25:201–09

32. Bulakbasi N, Guvenc I, Onguru O et al: The added value of the apparent diffusion coefficient calculation to magnetic resonance imaging in the differentiation and grading of malignant brain tumors. 2004, *J Comput Assist Tomogr* 28:735-46

33. Fan G, Deng QL, Wu ZH et al: Usefulness of diffusion/perfusion weighted MRI in patients with non-enhancing supratentorial brain gliomas: a valuable tool to predict tumor grading? 2006, *Br J Radiol* 79:652-658

34. H R Arvinda, C Kesavadas, P S Sarma et al Glioma grading: sensitivity, specificity, positive and negative predictive values of diffusion and perfusion imaging. *J Neurooncol* (2009) 94:87-96

35. Law M, Yang S, Wang H et al: Glioma grading: sensitivity, specificity and predictive values of perfusion MR imaging and proton MR spectroscopic imaging compared with conventional MR imaging. 2003, *AJNR Am J Neuroradiol* 24:1989-1998

36. Knopp EA, Cha S, Johnson G et al: Glial neoplasm: dynamic contrast-enhanced T2-weighted MR imaging. 1999, *Radiology* 211:791-798

37. Aronen HJ, Gazit IE, Louis DN et al: Cerebral blood volume maps of gliomas: comparison with tumor grade and histologic findings. 1994, *Radiology* 191:41-51
38. Sugahara T, Korogi Y, Kochi M et al: Correlation of MR imaging-determined cerebral blood volume maps with histologic and angiographic determination of vascularity of gliomas. 1998, *Am J Roentgenol* 171:1479-1486
39. Lev MH, Rosen BR: Clinical applications of intracranial perfusion MR imaging. 1999, *Neuroimaging Clin N Am* 9:309-331
40. Shin JH, Lee HK, Kwun BD et al: Using relative cerebral blood flow and volume to evaluate the histopathologic grade of cerebral gliomas: preliminary results. 2002, *Am J Roentgenol* 179:783-789
41. Lee KL, Seung HC, Tae JY et al Prediction of response to concurrent chemoradiotherapy with temozolomide in glioblastoma: application of immediate post-operative dynamic susceptibility contrast and diffusion-weighted MR imaging. 2015 *Korean J Radiol* 16(6)1341-1348
42. Kim JH, Choi SH, Ryoo I et al Prognosis prediction of measurable enhancing lesion after completion of standard concomitant chemoradiotherapy and adjuvant temozolomide in glioblastoma patients: applications of dynamic susceptibility contrast perfusion and diffusion weighted imaging. 2014 *PLOS ONE* November 24.
43. X. P. Zhu, K. L. Li, I. D. Kamaly-Asl et al. Quantification of endothelial permeability, leakage space, and blood volume in brain tumors using combined T1 and T2* contrast-enhanced dynamic MR imaging. *Journal of Magnetic*

Resonance Imaging, vol. 11, no. 6, pp. 575–585, 2000.

44. K.L.Li, X.P.Zhu, D.R.Checkleyetal Simultaneousmapping of blood volume and endothelial permeability surface area product in gliomas using iterative analysis of first-pass dynamic contrast enhanced MRI data. *British Journal of Radiology*, vol. 76, no. 901, pp. 39–50, 2003.

45. Roberts HC, Roberts TPL, Brasch RC, and Dillon DW Quantitative measurement of microvascular permeability in human brain tumors achieved using dynamic contrast- enhanced MR imaging: correlation with histologic grade. *American Journal of Neuroradiology*, vol. 21, no. 5, pp. 891–899, 2000.

46. Provenzale J.M, Wang G.R., Brenner T. et al Comparison of permeability in high-grade and low- grade brain tumors using dynamic susceptibility contrast MR imaging *American Journal of Roentgenology*, vol. 178, no. 3, pp. 711–716, 2002.

47. Mills S. J., Patankar T. A., Haroon H. A. et al Do cerebral blood volume and contrast transfer coefficient predict prognosis in human glioma? *American Journal of Neuroradiology*, vol. 27, no. 4, pp. 853–858, 2006.

